INVESTIGATION OF VELOCITY-BREAKTHROUGH RELATIONSHIPS IN CARBON FILTERS

Lyle L. Dauber
U.S. Army Soldier and Biological Chemical Command
Aberdeen Proving Ground, Maryland

David R. Peterson, P.E.
Science Applications International Corporation
Edgewood, Maryland

Carl A. Betten, P.E.
Science Applications International Corporation
Edgewood, Maryland

Kenneth W. Heffley
Flanders/CSC
Bath, North Carolina

Abstract

Using *performance* specifications (vice design specifications) the Army has acquired V-bed carbon filter cells of two types – some having 8 ea 1-3/8" carbon beds and others having 6 ea 2" carbon beds. The two types have an identical casing and an identical calculated residence time. Both have performed well. The purpose of this Army-sponsored investigation was to determine which of the two cells has the greater life and to identify the zone of earliest penetration.

Investigators determined time-to-breakthrough, T_b, and velocity, V, relationships for both cell types. They challenged each cell with 50 vppm R-11 at rated throughput, 1000 cfm. Breakthrough was defined as a downstream-upstream concentration ratio (C_d/C_u) of 0.10%. Investigators measured T_b and V in nine separate zones in each bed.

For both cell types, velocity profiles were fairly uniform throughout the leading 2/3 of the bed. The average velocity through the trailing 1/3 of the bed was somewhat less than in the leading portions. The lesser velocity through the trailing portion can be attributed to increased flow resistance as the flow channel narrows and adjacent beds converge.

From test data, cells with the thicker (2") beds outlasted the thinner (1-3/8") beds by a factor of two. For both type cells, breakthrough occurred earliest in the trailing portion of a bed where velocity was least. From velocity-breakthrough test data, for large beds one may arguably infer a near-direct relationship between V and T_b, i.e., the greater the velocity the longer the time to breakthrough. This inference is inconsistent with prevailing "breakthrough time" formulae. Using fluid dynamics principles, with special attention to the Coanda effect, investigators provide a theory for this inconsistency.

Introduction

The analysis of breakthrough is of interest to manufacturers and users of two major items: carbon filter canisters used in gas masks and larger high efficiency gas adsorber (HEGA) filters used in containment. Analysis of canister breakthrough is typically performed using the modified Wheeler equation, which gives the time to breakthrough as:

$$t_b = \frac{W_e}{QC_o}\left[M - \frac{\rho_B Q}{k_v}\ln\left(\frac{C_o}{C_x}\right)\right] \quad (1)$$

where t_b = breakthrough time, C_x = exit concentration at breakthrough, C_o = inlet concentration, Q = volumetric flow rate, M = weight of adsorbent, ρ_b = bulk density of packed bed, W_e = adsorption capacity (mass of adsorbed vapor/mass of adsorbent at concentration C_o), and k_v = rate constant.

Analysis of adsorbers used in bulk containment is usually performed in accordance with the requirements of the Code on Nuclear Air and Gas Treatment AG-1. Using variables consistent with the modified Wheeler equation (1), this code calculates the breakthrough time as:

$$t_b = \frac{W_e \rho_B A L_t L_z}{QC_o}[1 - f] \quad (2)$$

where A = effective bed face area, L_t = total bed depth, L_z = length of mass transfer zone (MTZ), and f = constant based on allowable C_x.

These two expressions give identical results, if: $M = \rho_B A L_t L_z$, and (3)

$$f = \frac{\rho_B Q}{Mk_v}\ln\left(\frac{C_o}{C_x}\right). \quad (4)$$

Both expressions are similar in that they express the breakthrough time as an estimated value related to the total quantity of carbon, reduced by a quantity proportional to the critical bed depth—the depth beyond which the breakthrough time is distinguishable from zero.

There are several problems with both expressions. For example, each expression is dependent upon several empirical quantities which disguise the true mechanics of gas movement. Further, the effect of adsorber cell geometry is not adequately addressed. Still further, the equations give no clue as to *where within a bed* breakthrough is most likely to first occur. The result of these problems is that currently manufactured cells are not as efficient as they could be. To achieve a guaranteed breakthrough time, excess carbon is used in the adsorber cell.

Objective

Under current Contract Number DAAM01-96-D-0009, Delivery Order (DO) 4-57, SAIC was tasked by the government to perform an engineering investigation of two types of carbon filters that have been used with the mobile igloo filter systems. The focus of this investigation was to: (1) determine whether 1 3/8-inch or 2-inch thick carbon beds provide the best filter performance, and (2) recommend any changes necessary to the procurement specification as a result of the investigation. SAIC was required to test both types of filters and collect velocity profile and gas penetration data across the filters and to assess the role that any edge effects or geologic faults have on filter performance. This report provides a summary of the filter testing.

Background

Under Contract Number DAA15-91-D-0005, DO 186, SAIC was tasked to design, procure, and deliver seven prototype igloo filter systems. SAIC developed the Igloo Filter Procurement Specification Number 4980-001 that identified the performance requirements for this transportable filter system. SAIC supplied seven filter systems through its subcontractor, Flanders/CSC. These trailer-mounted systems were capable of filtering 1,000 cubic feet per minute (cfm) of air. Each filter system consisted of a prefilter, a high efficiency particulate air (HEPA) filter, and two carbon adsorber filter cells. These filter systems required a filter cell with eight carbon-filled beds that were 1 3/8-inch thick, hereafter called 1 3/8-inch cells. Subsequently, under Contract Number DAAM01-96-D-0009, DO 4-13, SAIC was tasked to supply 36 additional filter systems. For these filter systems, the government required a

filter cell that had six carbon-filled beds that were 2-inches thick, hereafter called 2-inch cells. At that time, the procurement specification for the filter systems was revised and has continued to specify 2-inch cells. Each cell is a sealed stainless steel box that is used to direct the air flow through the carbon beds. The carbon adsorbs or captures undesirable gases. Inside the filter cell are V-shaped beds made of stainless steel screen that secure the carbon in place. The filters used for the mobile filter system use a coarse grained (8 X 16 mesh) activated carbon made from coconut shells. The cells are designed to pass a certain quantity of air at a prescribed pressure drop across the filter. In addition, each filter cell has a prescribed residence time to ensure that the filter beds have adequate time to adsorb the undesirable gases. The 1 3/8-inch and 2-inch filter cells have identical exterior dimensions of 24-inches high, 24-inches wide, and 16-inches deep. Figure 1 shows a typical filter cell.

The 1 3/8-inch cell is designated as model number CSC-16-81-3/8-AS and the 2-inch cell is designated as model number CSC-16-62-AS. Vendor literature for the CSC-16-81-3/8-AS estimates a residence time of 0.125 second and an approximate pressure drop of 0.85 inch water gauge at 1,000 cubic feet per minute (cfm). For the CSC-16-62-AS, a residence time 0.125 second and an approximate pressure drop of 1.45 inches water gauge at 1,000 cfm are estimated. The CSC-16-81-3/8-AS has eight beds and holds about 76 pounds of carbon and the CSC-16-62-AS has six beds and holds about 80 pounds of carbon. Based on a comparison of the vendor literature, it appears that the 1 3/8-inch filter cells should have better filter performance than the 2-inch cell. The lower pressure drop and associated reduced flow velocity through each bed should produce more uniform gas penetration and make the 1 3/8-inch cell less susceptible to premature failure. Figures 2, 3, 4, and 5 show details of the two types of filter cells.

Test Location
The testing was performed at the Flanders/CSC facilities located in Bath, North Carolina. The tests were conducted in a building used to check the performance of production filters.

Test Schedule
Testing occurred on January 25, 26, 27, and 28, 2000. On January 25 and 26, full penetration testing was performed. On January 26, 27, and 28, velocity and local penetration testing were performed. Non-destructive radiographic testing was performed on January 26 and 27.

Equipment
Two sets of test equipment were used. The first set of test equipment was supplied by Flanders/CSC to measure the filter adsorption and flow performance. It included production quality filter cells, wind tunnel test structure, and related test instrumentation. Figure 6 shows the wind tunnel test structure.

The second set was supplied by Precision Calibration and Testing (PCT) to perform nondestructive examinations of the filter cells to check for potential internal faults. The PCT equipment included a portable X-ray system and mobile X-ray film development unit.

Instrumentation
Two sets of instrumentation were used for the flow tests. The first set measured halide concentrations both upstream and downstream of the filter. It included a gas chromatograph, a continuous halide monitor strip chart recorder, sampling wedges, and a 10 port sampling valve. The second set measured the velocity distribution of air within the filter cell. It included a differential pressure transmitter, sampling wedges, and a 10 port sampling valve.

Test Procedure
The filter performance investigation was divided into four phases. Phase I – Breakthrough tests – involved measuring the total halide breakthrough times for both the 1 3/8-inch cells and 2-inch cells. Phase II – Velocity distribution tests – involved measuring the velocity inside discrete flow zones of the filter bed. Phase III – Breakthrough distribution tests – involved measuring the halide concentrations within discrete zones of the filter cell. Phase IV – Radiographic tests – involved nondestructive examination of the filter cells that were tested in phases 1, 2, and 3.

a. *Phase I – Breakthrough Tests.* These tests involved two 1 3/8-inch cells and two 2-inch cells. They were run to determine the time for a whole filter cell to incur halide breakthrough. Breakthrough is defined as the point when concentration levels downstream of the filter reach a prescribed level. For these tests, a downstream value of 0.1 percent of the upstream concentration was prescribed as the breakthrough point. Trichloromonofluoromethane, commonly called R-11, gas was used as the halide. The tests run, and procedures used, were as follows:

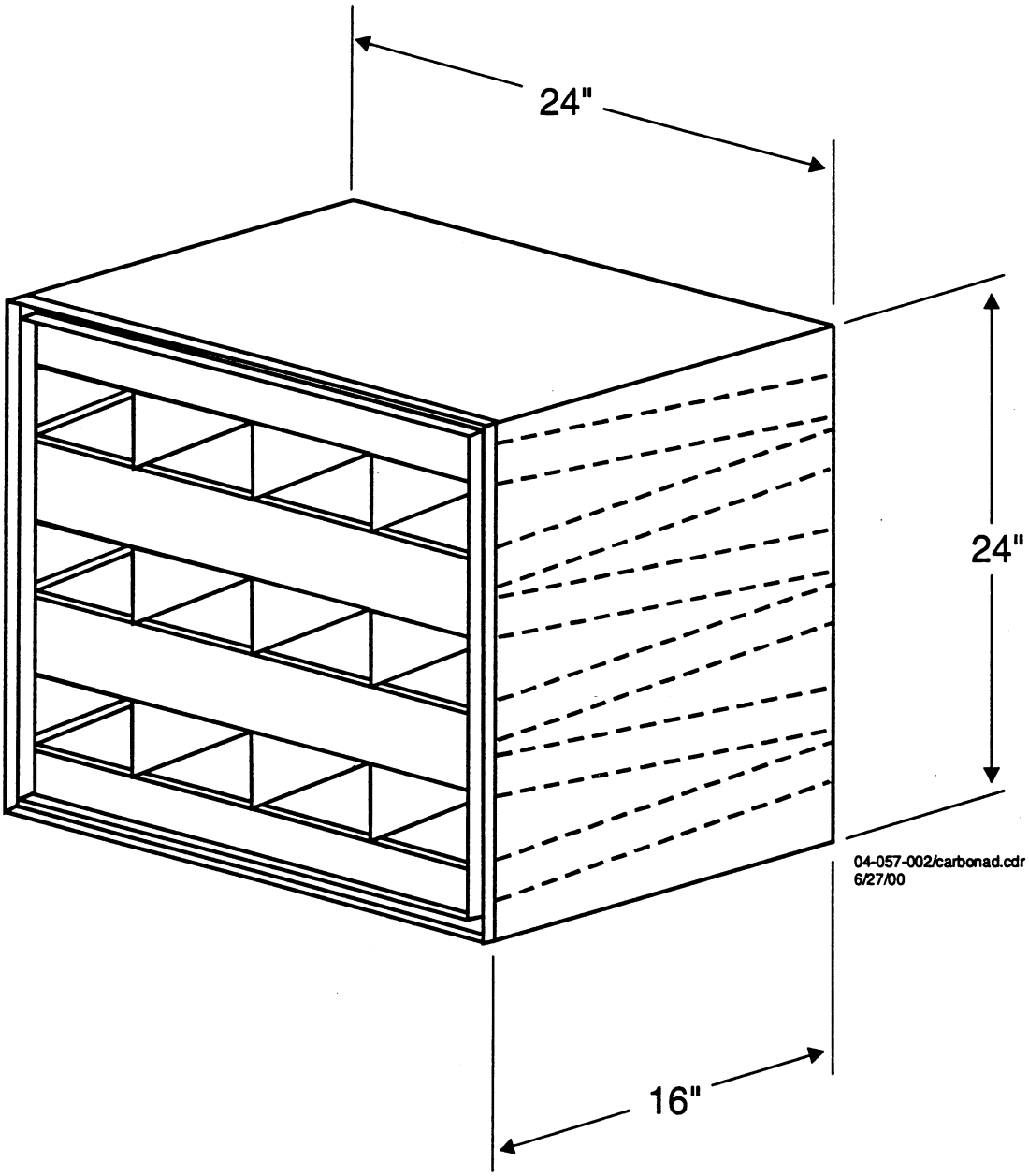

Figure 1. Typical Carbon Adsorber Filter Cell

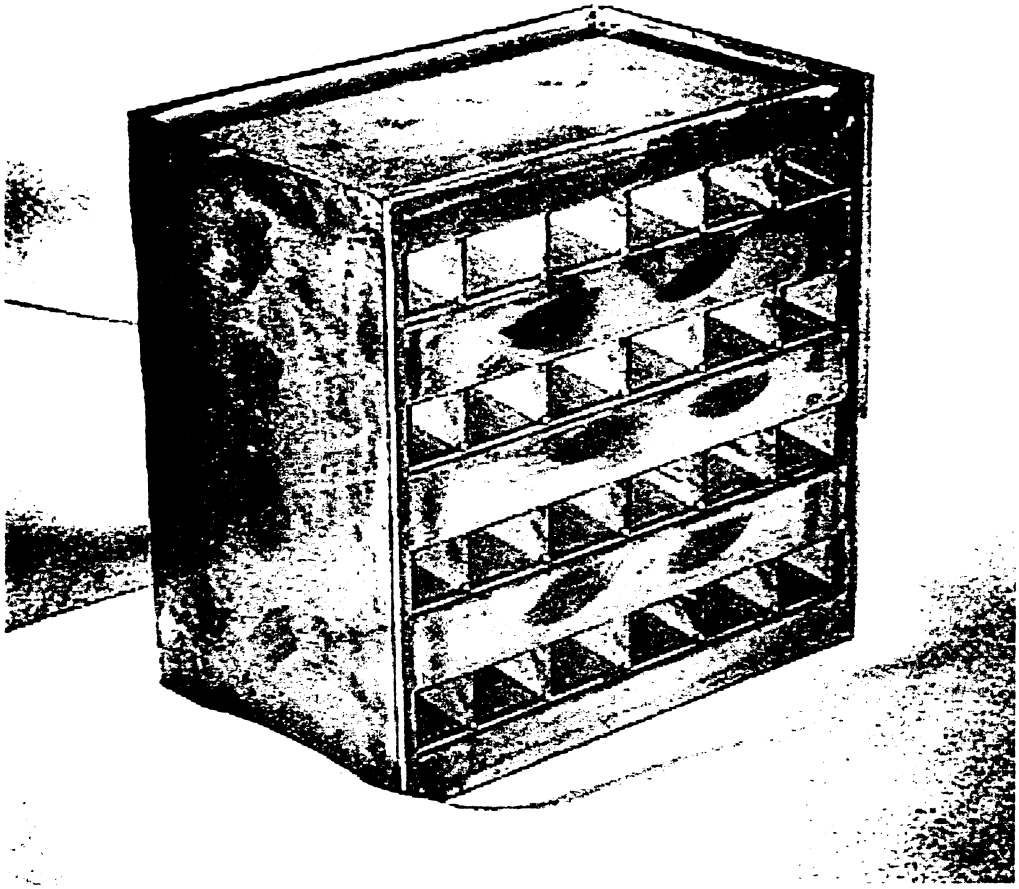

Figure 2. Front View of 1 3/8-inch Filter Cell

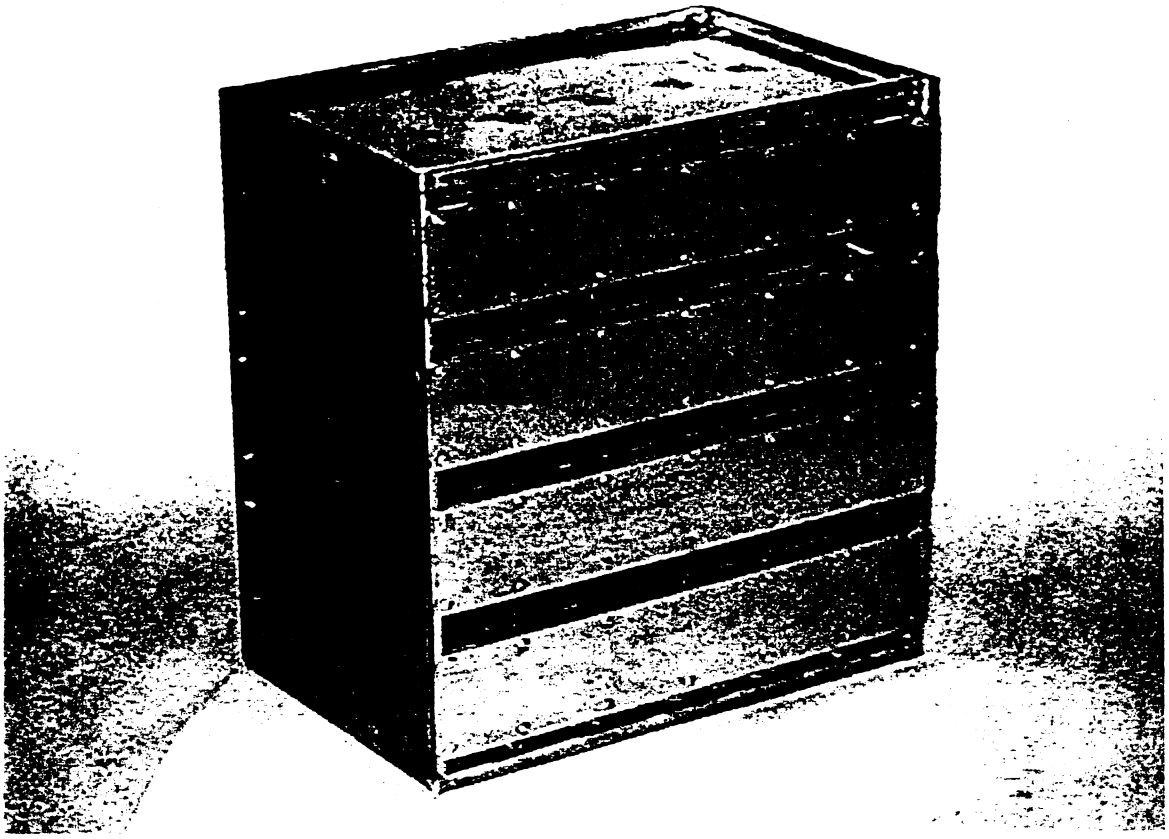

Figure 3. Rear View of 1-3/8 Filter Cell

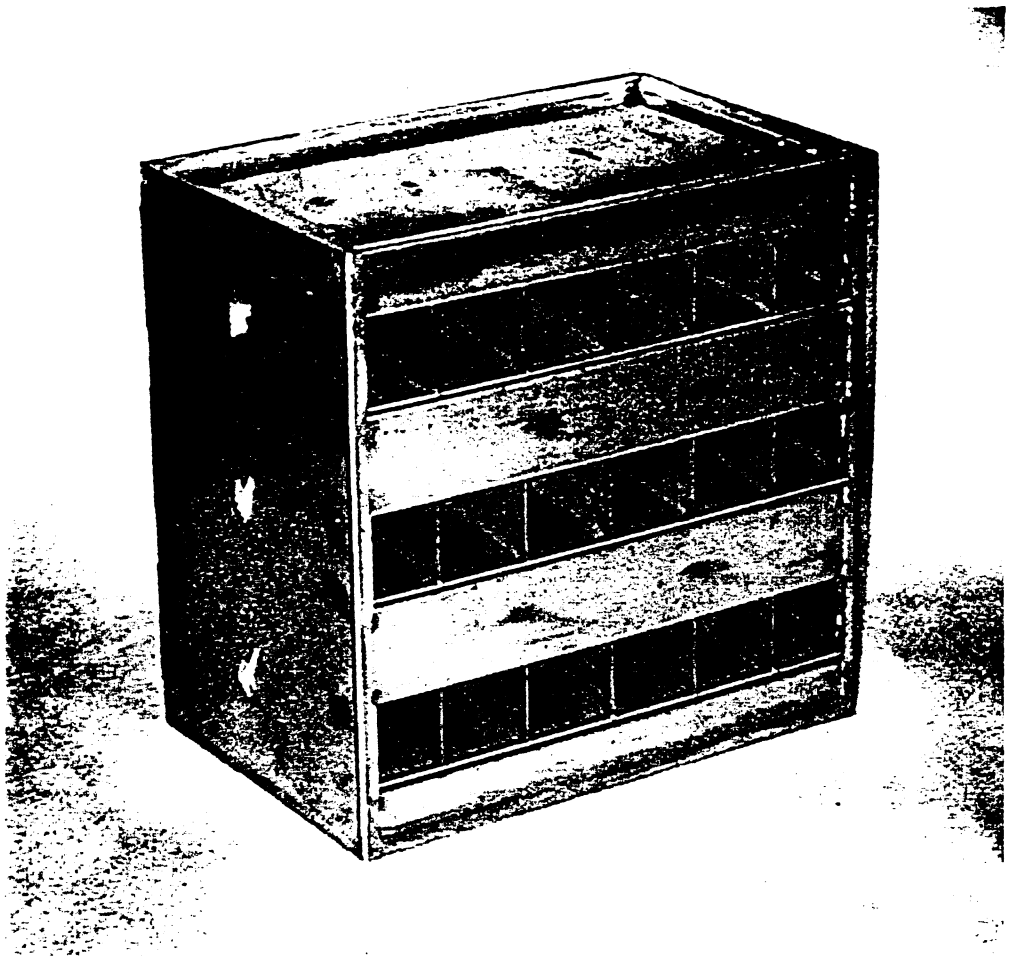

Figure 4. Front View of 2-inch Filter Cell

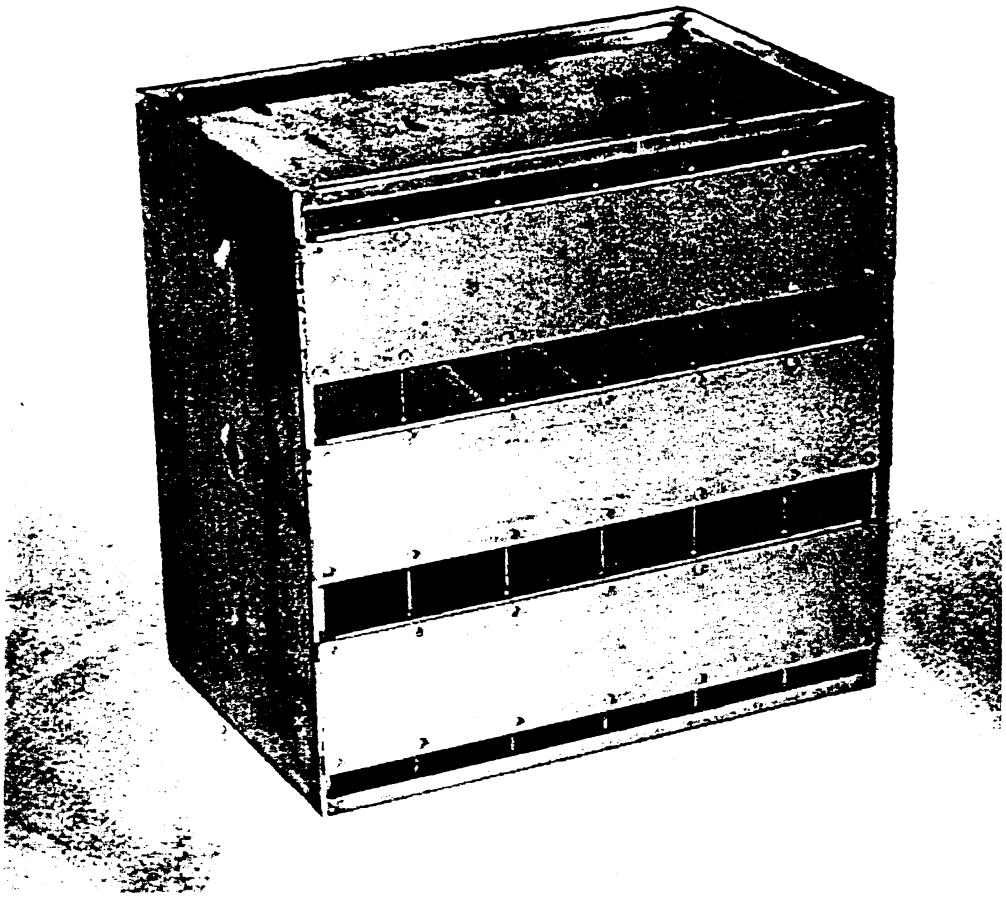

Figure 5. Rear View of 2-inch Filter Cell

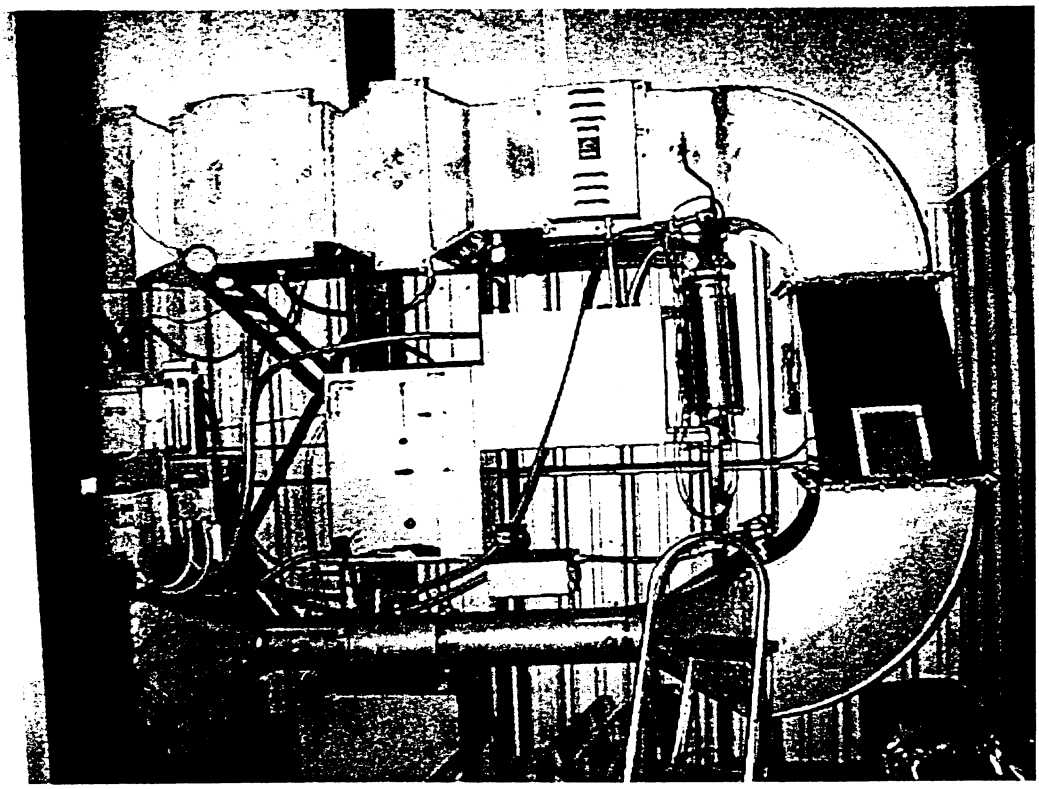

Figure 6. Wind Tunnel Test Structure

- *Run 1.* The 2-inch cell was mounted in the wind tunnel. Two tubes, one upstream and one downstream of the filter, were connected to a gas chromatograph. The flow was set at 1,000 cfm and the upstream halide concentration was set at 50 parts per million (ppm). During the test, halide concentrations upstream and downstream of the filter were measured and recorded on a strip chart. The time was recorded to determine the exact moment when the downstream concentration exceeded 0.05 ppm.

- *Run 2.* The Run 1 setup and testing procedure was used except that the 1 3/8-inch cell was used.

- *Run 3.* The Run 1 setup and testing procedure was used except that a second 1 3/8-inch cell was used.

- *Run 4.* The Run 1 setup and testing procedure was used on a second 2 inch cell.

b. *Phase II – Velocity Distribution Tests.* These tests involved two 1 3/8-inch cells and two 2-inch cells. These tests determined the velocity distribution within each type of filter cell. The test runs and procedures used were as follows:

- *Run 5.* The 1 3/8-inch filter was mounted backward in the wind tunnel. The backward mounting was necessary to permit the sampling wedges to be located on the downstream side of the filter. The sampling wedges were mounted in all openings of the filter cell to balance the flow. Velocity measurements were taken from two of the eight beds. Nine tubes were connected to the sampling wedge, and then to the 10 port sampling valve. The output line from the valve went to the differential pressure transmitter. Figures 7, 8, and 9 show details of the sampling wedges. The face of the five beds not fitted with the sampling wedges was taped closed with duct tape. The flow was set at 375 cfm (3/8 × 1,000) to produce rated flow through each bed under examination. During the test, the velocities in the sampling wedges were measured at discrete time intervals by rotating the 10 port valve and recording the data manually. After the nine sets of velocity data were recorded, the test fixture was shut down, and the nine sampling tubes were moved over to another set of sampling wedges. Setup was replicated and velocity data were then recorded for the new zones. This procedure was repeated for all the sampling wedge locations (zones).

- *Run 6.* The same setup and testing as Run 5 was used except that the 2-inch cell was used. The sampling wedges were placed in three of the six beds of the filter cell. The face of the beds not fitted with the sampling wedges were taped closed with duct tape. The flow was set at 500 cfm (3/6 × 1,000).

- *Run 7.* The Run 5 setup and testing was used.

- *Run 8.* The Run 6 setup and testing was used.

c. *Phase III – Breakthrough Distribution Tests.* These tests involved the same two 1 3/8-inch cells and two 2-inch cells that were used in Phase II tests. This test was run to determine the exact zones within the filter cell where breakthrough first occurs. For this test, only three sampling wedges were used to obtain test data. The test runs and procedures used were as follows:

- *Run 9.* The 1 3/8-inch filter was mounted backward in the wind tunnel. The backward mounting was necessary to permit locating the sampling wedges on the downstream side of the filter. The sampling wedges were mounted in three of the eight beds of the filter cell. In the openings where measurements were not taken the openings were filled with wedges to balance the flow. The nine tubes were connected to three sampling wedges and to the 10 port sampling valve. The output line from the valve went to the gas chromatograph. The five beds not fitted with the sampling wedges were taped closed with duct tape. The flow was set at 375 cfm and the upstream halide concentration was set at 50 ppm. During the test, the halide concentrations upstream and in the three sampling wedge locations were measured by rotating the 10 port valve and recorded on a strip chart. The locations where the downstream concentrations exceeded 0.05 ppm were noted.

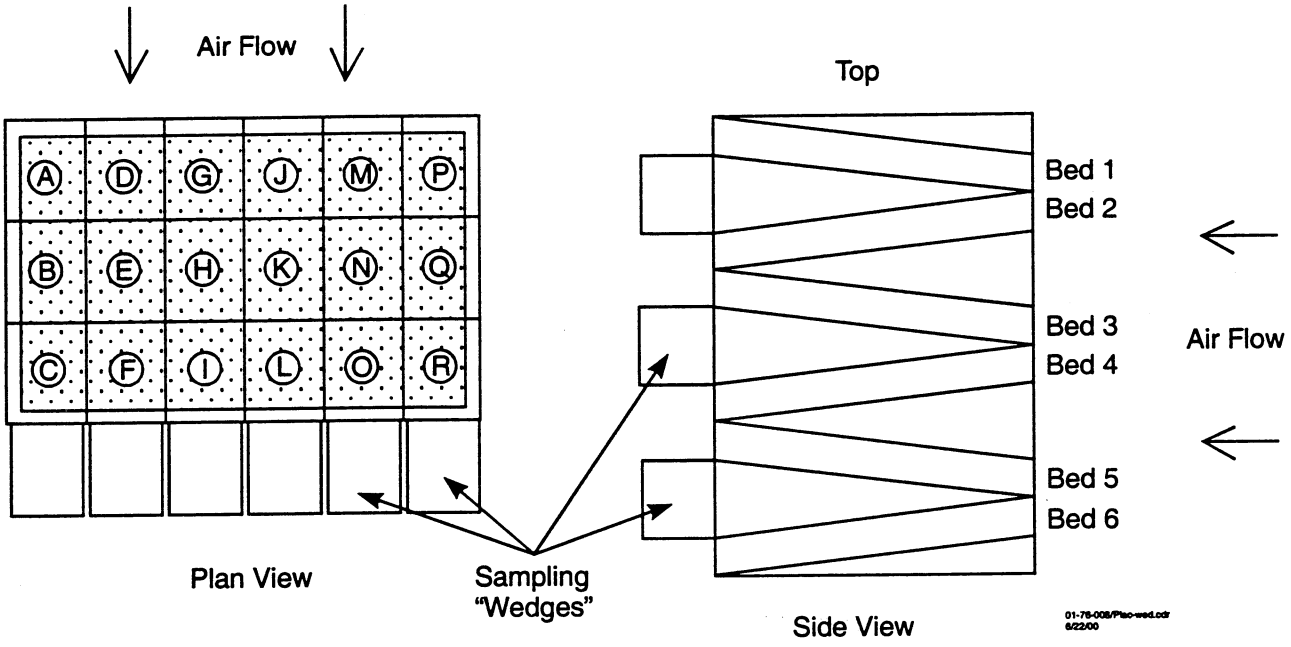

Each "Wedge" will allow sampling of 6 points (3 each from adjacent beds).

Figure 7. Placement of Sampling Wedges in Filter Cell

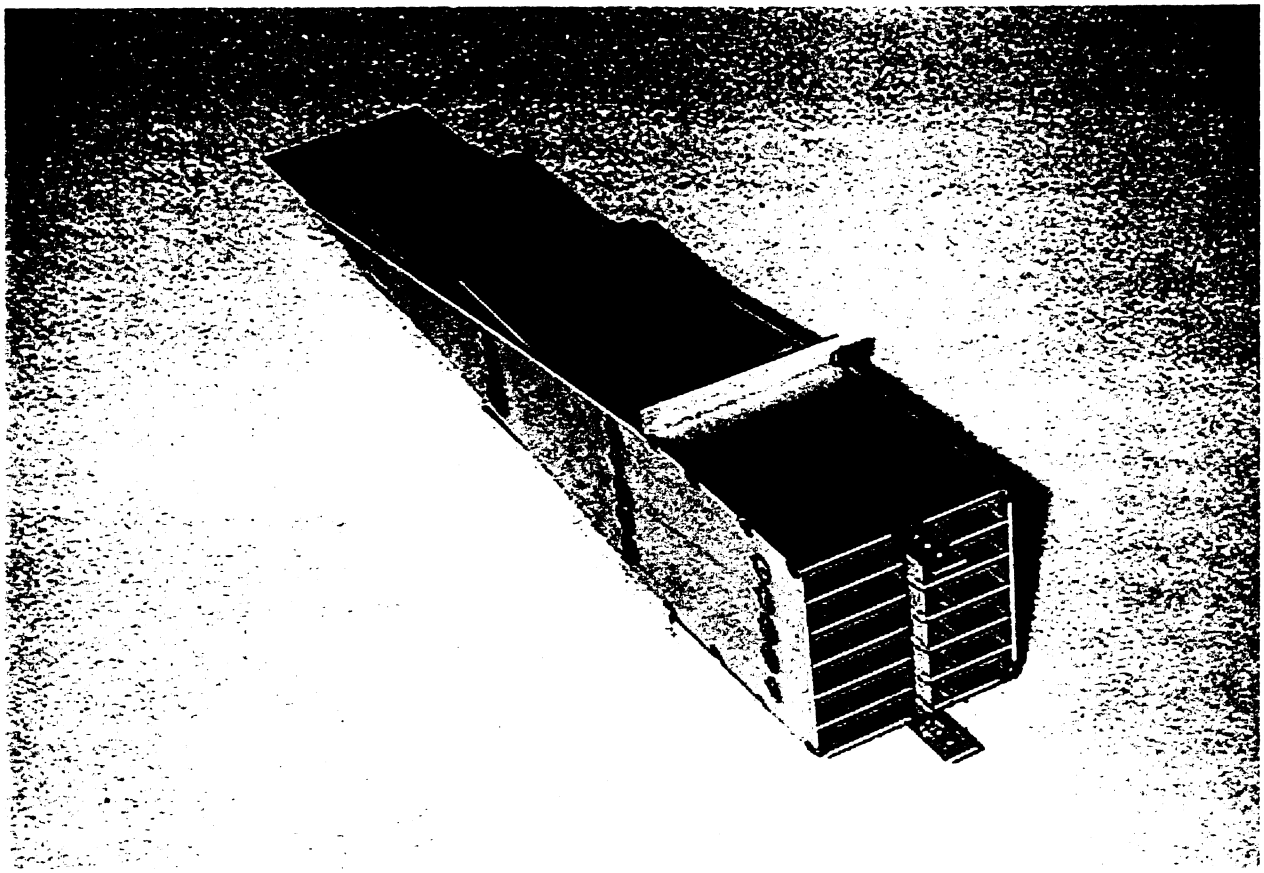

Figure 8. Typical Sampling Wedge

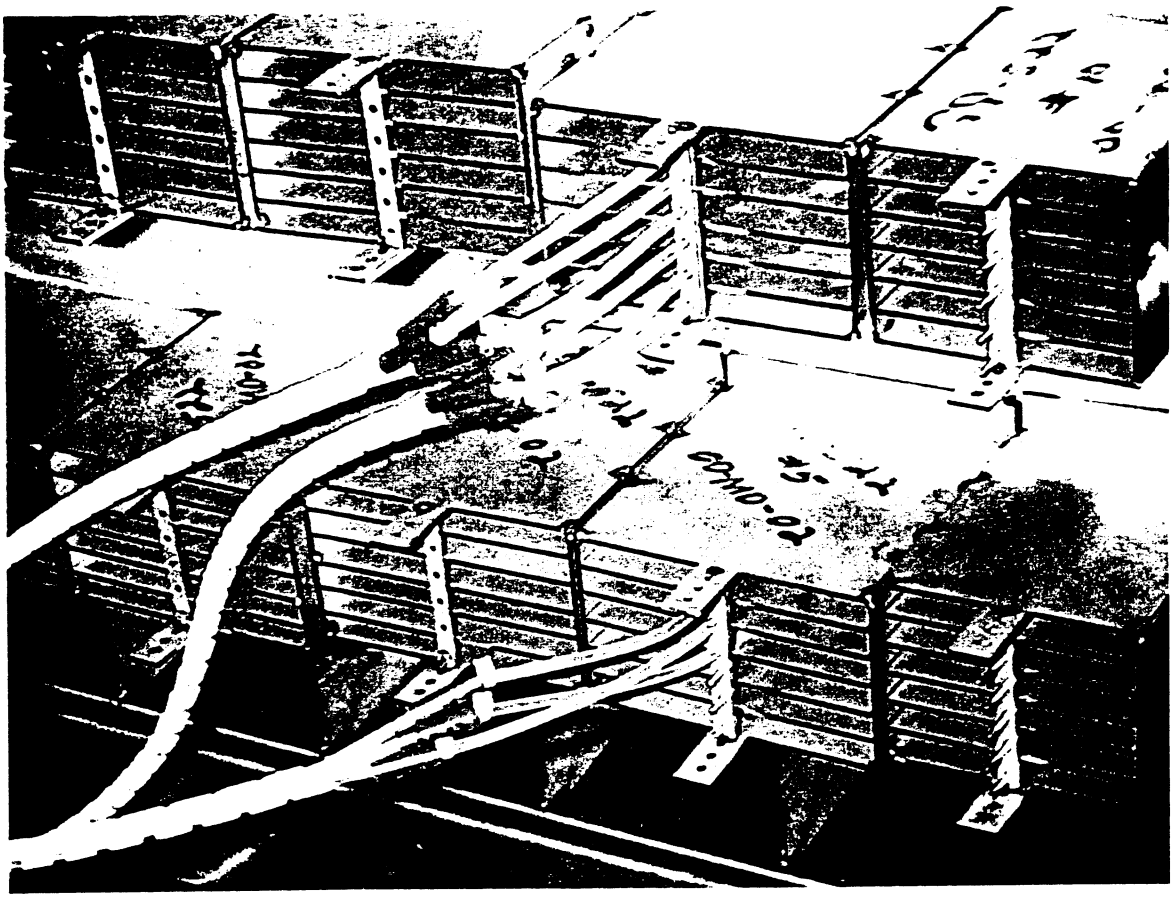

Figure 9. Sampling Wedges Installed in Filter Cell

- *Run 10.* The same setup and testing used in Run 9 was used except that the 2-inch cell was used. The sampling wedges were placed in three of the six beds of the filter cell. The beds not fitted with the sampling wedges were taped closed with duct tape. The flow was set at 500 cfm.

- *Run 11.* The Run 9 setup and testing was used.

- *Run 12.* The Run 10 setup and testing was used.

d. Phase IV – Radiographic Tests. These tests involved the radiographic examination of the same four 1 3/8-inch cells and four 2-inch cells that were used in the Phase 1, 2, and 3 tests. These nondestructive tests were performed to examine each filter cell to determine if there were any perceptible geological faults in the filter cell. The test runs and procedures used follow:

- *Phase 1 Cell Examinations.* The two 1 3/8-inch and two 2-inch filter cells that were used for the total halide breakthrough tests were placed in a restricted area where an X-ray source could be safely used. Unexposed photographic film was placed in one row of the filter cell. An X-ray source was then activated to expose the film. Figure 10 shows the portable X-ray test setup. This procedure was repeated for each row until the complete filter cell was examined.

- *Phases 2 and 3 Cell Examinations.* Investigators used the same setup as that used for Phase 1 cell examinations. These examinations focused only on the three beds adjacent to the sampling wedges.

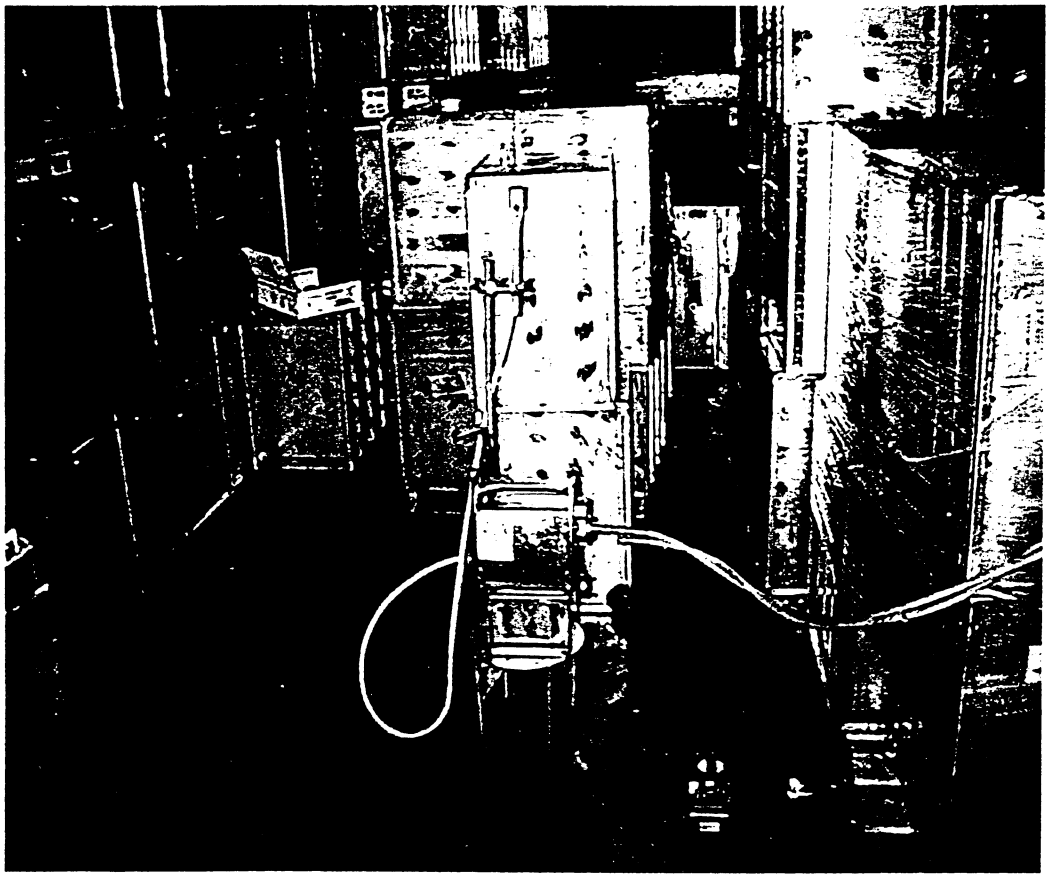

Figure 10. Portable Radiographic Test Setup

Results

Breakthrough Results

These tests were performed to obtain whole cell breakthrough data for both 1 3/8-inch and 2-inch filter cells. Both types of cells were exposed to 1,000 cfm of air laden with a 50 ppm concentration of halide. Breakthrough was defined as the point when the downstream halide concentration exceeded 0.1 percent of the upstream concentration, that is, 50 ppb. The results of these tests are shown in table 1. The average breakthrough time for the two 1 3/8-inch filter cells was 1.04 hours. For the two 2-inch filter cells, the average breakthrough time was 2.46 hours. Based on these tests it appears that the 2-inch cell will last more than twice as long as the 1 3/8-inch cell. Statistical analysis of these results indicate that at the 95 percent confidence level, the breakthrough times for the 2-inch cell are at least 40 minutes longer than the 1 3/8-inch cell.

Table 1. Whole Cell Breakthrough Time Test Results

Run No.	Cell Size	Breakthrough Time - Minutes	Carbon per Cell-pounds	R-11 Adsorbed Ounces
1	2 inch	135	81	39.3
2	1 3/8 inch	69	77.5	19.7
3	1 3/8 inch	56	76.5	19.7
4	2 inch	160	82.5	49.2

Velocity Distribution Results

These tests determined airflow velocity distribution within each filter bed. Each filter bed was divided into zones, and the airflow velocity of each zone was measured. Velocity distributions were measured on three of the filter beds. For the 1 3/8-inch cell, three of the eight beds were sampled, so the air flow was set at 375 cfm (3/8 × 1,000 cfm). Three of six beds for the 2-inch cell were sampled; therefore, the flow was set at 500 cfm (3/6 × 1,000 cfm).

Due to the invasive nature of the test setup, the measured flow velocities are not the superficial bed velocities seen under normal operating conditions. The recorded flow velocities are intended to provide a comparison of velocity variation between types of filters and cell locations. The velocity results are contained in appendix B. Figure 11 shows the velocity distribution data for bed 2 of a 2-inch filter cell.

Breakthrough distribution results

The breakthrough distribution tests were performed to determine the locations within the filter bed where breakthrough first occurs for each filter cell type. The tests were similar to those performed in the velocity distribution tests. The upstream air flow contained a 50 ppm concentration of halide, the flow for the 1 3/8-inch cell was set at 375 cfm, and the flow for the 2-inch cell was set at 500 cfm. The results for the same 2-inch cell as was used to generate figure 11 are shown in figure 12. For both types of cells, the earliest breakthrough occurred at the innermost portion of the V bed. These results are remarkable because the earliest breakthrough occurred where the velocity was lowest (at a wall), rather than the reverse.

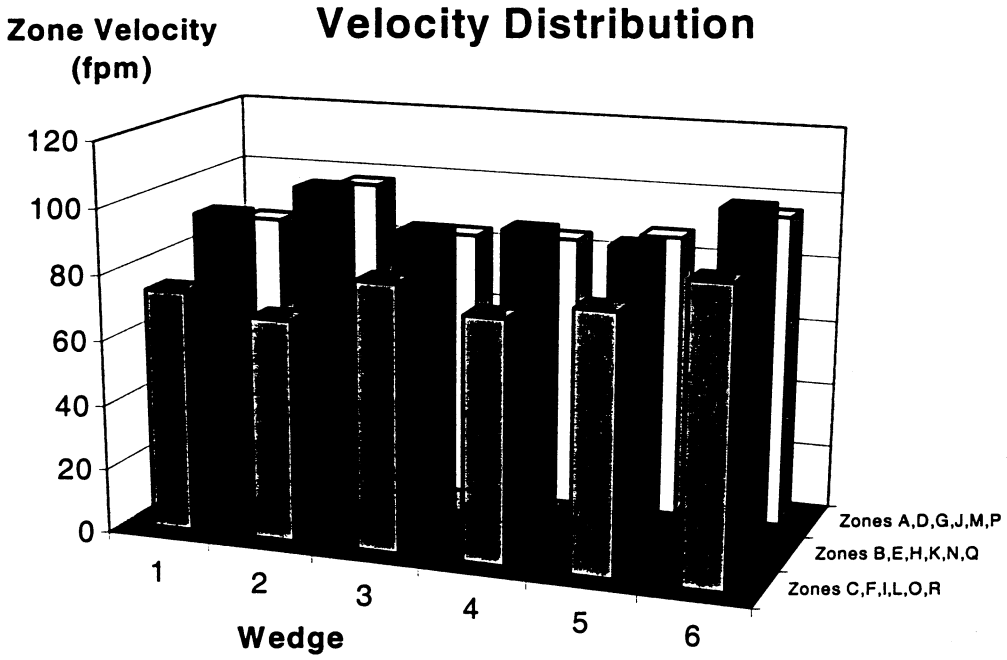

Figure 11. Typical Velocity Distribution for 2-inch Filter Cell

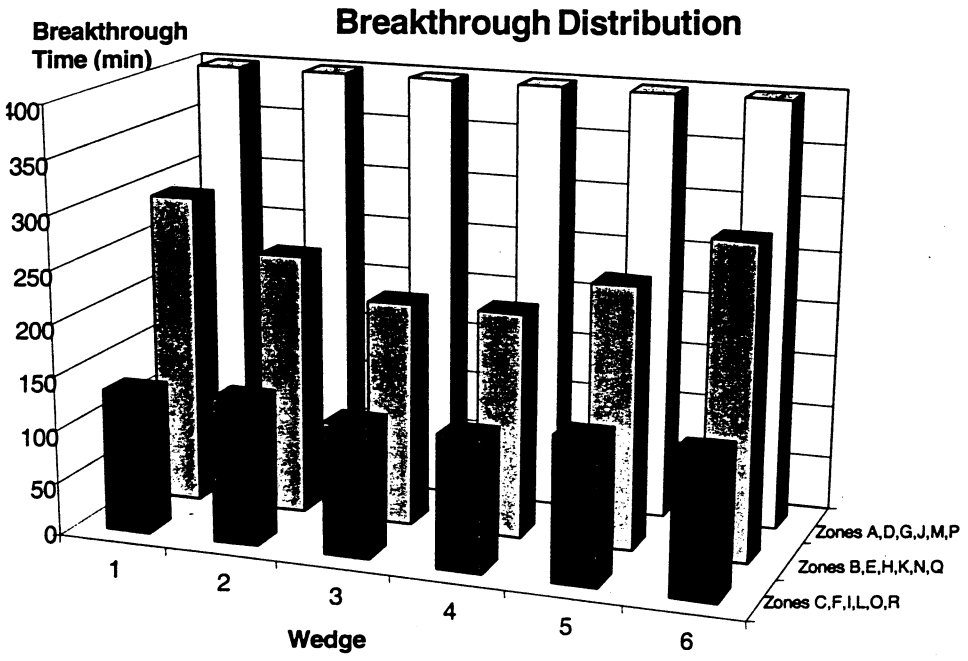

Figure 12. Breakthrough Distribution Results for 2-inch Filter Cell

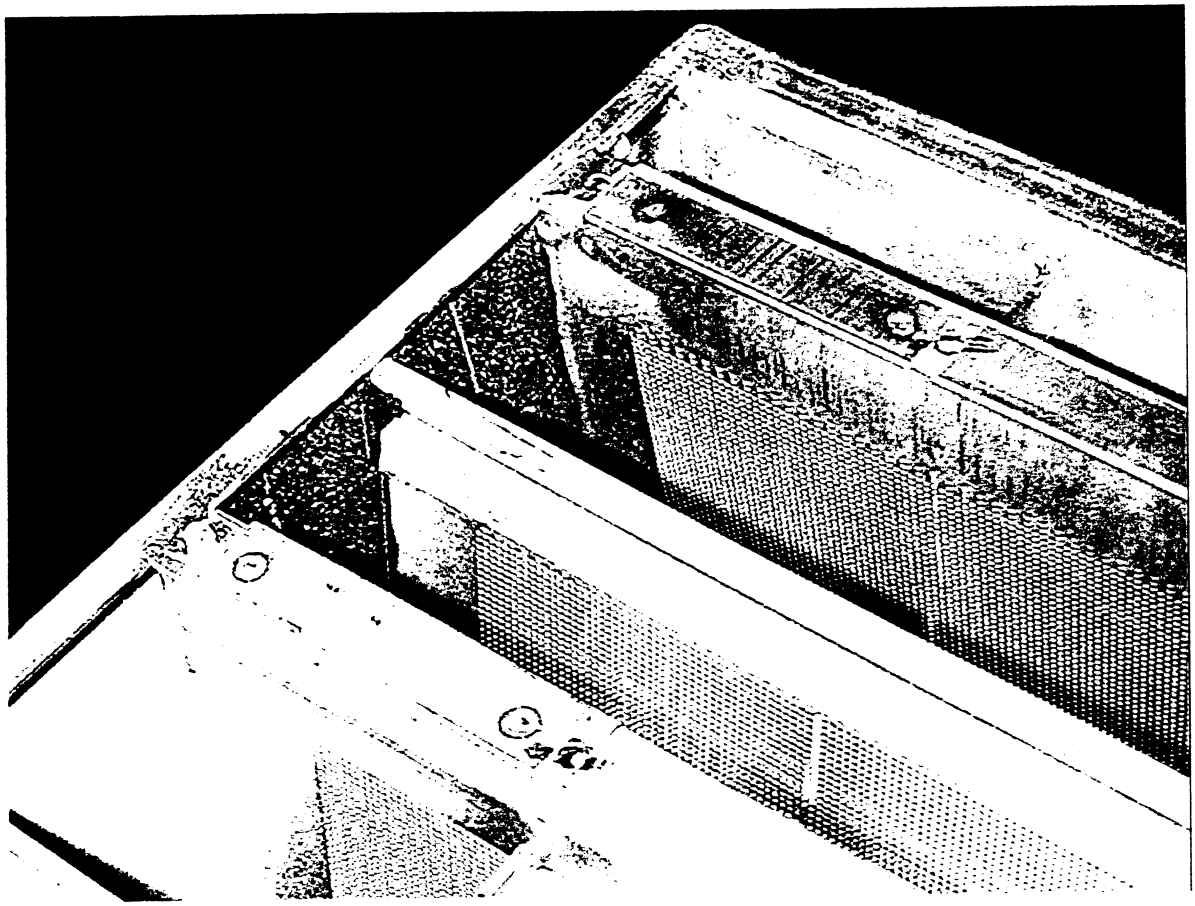

Figure 13. Filter Cell Edge Detail

Radiography Results

The radiography tests examined the same four 1 3/8-inch cells and four 2-inch cells that were used in Phase 1, 2, and 3 tests. These nondestructive tests were performed to determine if there were any perceptible geological faults in the filter cell, or if there were a correlation between density and adsorption performance. For the four filter cells used for the total halide breakthrough, the complete cell was X-rayed. The film from these cells was examined by the radiographic technicians. No geological defects were found. The same procedure was repeated for the four cells used for the local penetration tests. The technicians found no geological defects. Radiographic examinations are most effective when there are distinct density differences between materials. For the filter cells, stainless steel is the densest material and is distinctly shown as white areas in the developed photographic film. Carbon is the least dense material and is shown as black areas. To check how well voids in the carbon beds will be shown, a test was performed on a sample filter cell. Styrofoam pieces of varying size and thickness were placed within the sample filter cell. The voids created by the Styrofoam were clearly visible in the film. Other dense items such as pop rivets were also visible on the film. Small voids or other geological faults in the carbon beds were not detectable by

radiographic examination. Overall, it was concluded that radiographic examination is not a practical method of locating geologic faults within the carbon beds. During this test phase, the method of fabricating the filter cells was examined. This was done to determine if air can bypass the carbon beds by leaking around the edges of the carbon beds. The filter cell consists of an outer stainless steel skin and internal V-shaped stainless steel screens. The screens are used to contain the granular carbon. The screens are welded to the filter skin and a layer of polyurethane is used to prevent carbon from spilling from the bed. Also, the holes in the screens do not go all the way to the outer edge of the filter skin. This screen design causes pockets at the filter edges where the airflow becomes trapped. It was concluded that the construction of the filter cell minimizes any reasonable likelihood that gases will bypass the bed. Figure 13 shows the filter cell edge details.

Discussion

Previous sections discussed test results that illustrated some shortcomings in the classical methods of analyzing breakthrough. Among the methods discussed are the modified Wheeler equation and the AG-1 equation in section 1. As shown in figures 11 and 12, the velocities and breakthrough times seen in individual zones of a particular filter showed a general relationship, viz., the greater the velocity the longer the time to breakthrough. This *direct* relationship was contrary to the values predicted by equations 1 and 2, which indicate an *inverse* relationship.[1] This unanticipated outcome has been noted by other authors, notably Battelle [DTIC Report ARSL CR-80032] and Busmundrud [Carbon (1993), 31(2), 279-86], in large filter tests. There are several possible explanations for this unanticipated outcome. The authors give two explanations that are based in part on test data and in part on known fluid[2] mechanics principles, viz: (1) the inadequacy of bulk transport equations, and (2) the prominence of the Coanda effect in gas flow through carbon beds.

The inadequacy of bulk transport equations

Bulk transport equations provide the starting point for filter system design – identifying needed throughput and residence time, for example. Classical fluid dynamics texts rightly limit the application of the throughput formula $Q = AV$ to flow in *open ducts and pipes.* By inference, residence time (RT) – the elapsed time a fluid particle[3] will *reside* in a given space (RT = 1/V x distance traveled) – would also be limited to flow in open ducts and pipes. In these formulae, *average* velocities are required. These velocities are easily obtained for a filter system by taking point-by-point measurements across the inlet or exit duct. Readings are generally fairly uniform (wall regions excepted) in the ducts. On the other hand, velocities *in the carbon itself* can vary widely. In the small pores or pathways through which the gases must pass, velocities are great at a pathway's centerline, zero at its wall, and its direction is constantly changing. Further, the narrowness of the pathways places each fluid particle at or near a boundary where it may encounter friction or other forces. Moreover, at a bed's steel walls velocity goes to zero. It follows, therefore, that for large beds – beds with a large aspect ratio (thickness/width or breadth) – simple bulk transport equations that use measured exterior data are inadequate. They give no clue as to *where and when* a particular gas particle will break through.

The Coanda effect

The Coanda effect, described in classical fluid dynamics literature and prominent in commercial fluidic control systems, is believed to play a prominent role in gas adsorption in carbon. Its outworking in a carbon bed is described in figure 14. In short, moving fluids tend to hug a solid body and form streamlines that alter the course of some of the fluid particles. In carbon beds, the streamlines will tend to move fluid particles into lateral pathways or pores. The greater a particle's velocity the more kinetic energy it possesses and the deeper it will move into a lateral pathway or pore. There, opposing forces (e.g., friction and van der Walls forces) will cause some particles to come to rest. For a particular gas particle (e.g., a contaminant), the greater its velocity the deeper it will penetrate the pore before it is stopped. Thus, increased velocity could increase the efficiency of the adsorbent.

---

1 Since $Q = AV$, increased velocity (V) gives a larger value of Q which, in equations 1 and 2, makes t_b smaller. This equation assumes constant density and unidirectionality.

2 A *fluid* can be a liquid, gas, or visco-elastic substance (e.g., syrup). In this paper, fluid always refers to a gas.

3 *Fluid particle* is a term used in fluid mechanics literature to speak of a small number of molecules occupying an infintesimal control volume.

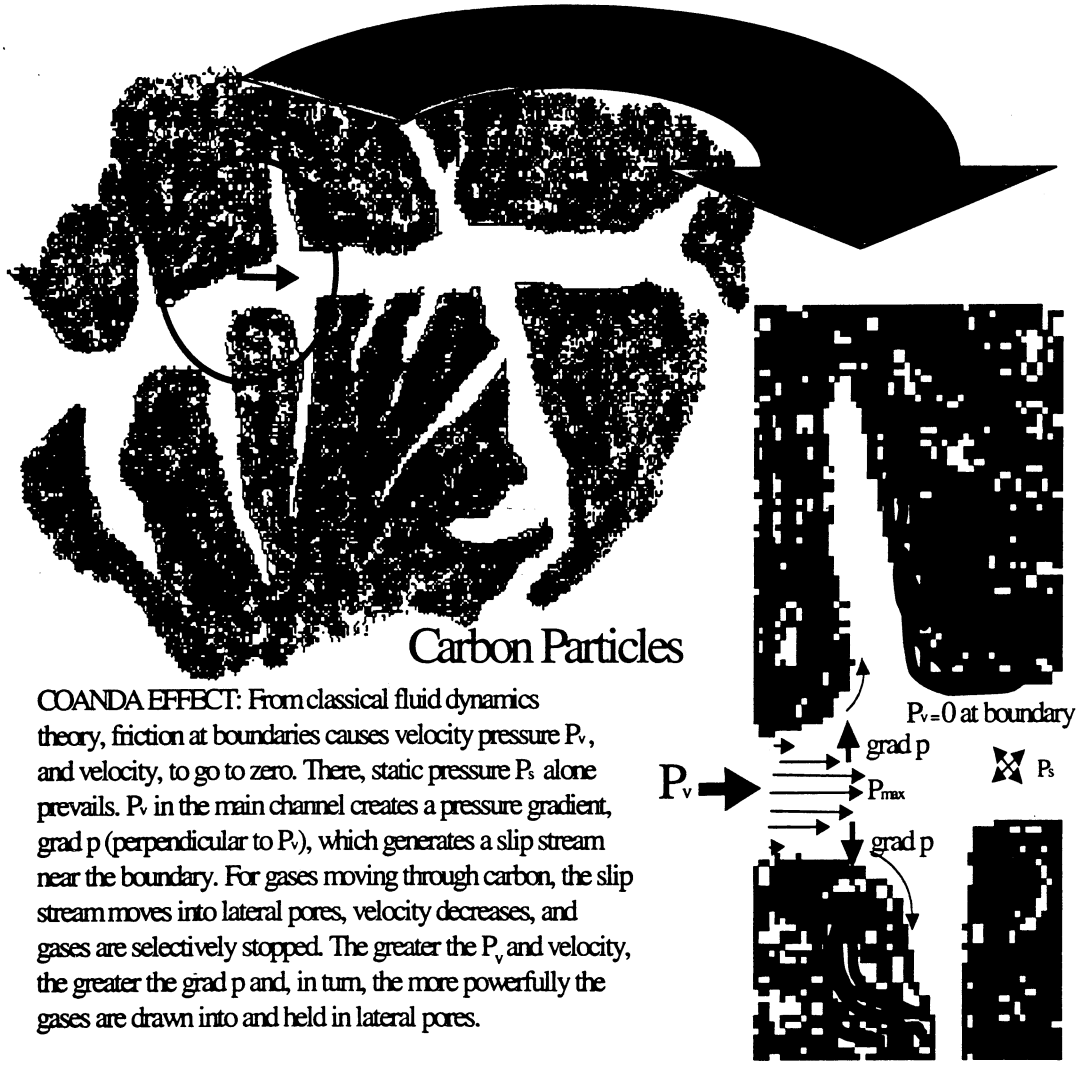

Figure 14. The Coanda Effect for Gases Moving in Carbon

For the tests at hand, the collection of breakthrough data by *zone* rather than at *numerous specific points* precluded investigators from identifying a more precise pattern of penetration of the challenge gas, R-11. From the foregoing discussion, however, one can infer that the adsorption process would be least efficient and breakthrough would be earliest near the steel walls of the bed where velocity goes to zero. For the tests in question, breakthrough came earliest in the region of a particular bed wall – the wall closest to the inlet V-point. HVAC principles would dictate that velocity would here be least. (Tapered ducts are rarely taken to a V-point owing to flow loss due to friction). Further work is needed to more precisely map velocities, loci and timing of breakthrough, and their relationships. The tests disclosed that a large portion of a bed is only partially penetrated when breakthrough first occurred. This outcome suggests that design and operating refinements may be possible that would lengthen the time to breakthrough and give a longer filter service life.

These test results, which consistently showed earliest breakthrough in the trailing portion of the bed where velocity was less than in the leading portions, are consistent with the *Coanda effect* principle. The collection of breakthrough data by *zone* rather than at *specific points* precluded investigators from identifying whether full penetration occurred first precisely at the steel wall.

Conclusions

a. The filter cell with six beds that are 2-inches thick gives a longer time to breakthrough than does a cell with eight beds that are 1-3/8 inches thick.

b. The location where local breakthrough occurs is in the innermost portion of the V bed.

c. The air velocities through, and pressure drop across, a 1 3/8-inch filter cell are smaller than for a 2-inch filter cell.

d. The filter system procurement specification does not have to be revised since it currently identifies the six bed 2-inch filter cell.

e. For large flat carbon beds, breakthrough occurs first at walls where velocity is least.

f. Radiographic examination of carbon filled filter cells is not a practical method of locating geologic faults within the filter beds.

g. Further investigation is needed on filter performance owing to edge effects, bed size and configuration, and velocity-breakthrough relationships.

APPENDIX A
ACRONYMS/ABBREVIATIONS

A	area
cfm	cubic feet per minute
DO	delivery order
FP	fluid particle
grad p	pressure gradient
HEGA	high efficiency gas adsorber
HEPA	high efficiency particulate air
KE	kinetic energy
MTZ	mass transfer zone
PCT	Precision Calibration and Testing
ppb	parts per billion
ppm	parts per million
P_s	static pressure
P_v	velocity pressure
Q	flow rate
SAIC	Science Applications International Corporation
V	velocity

APPENDIX B
TEST DATA

Table B-1. Flow Velocities for the First 1 3/8-inch Cell [CSC-16-81-38-A (1)]

Sample Zone	Bed 1 Velocities Feet per Minute	Bed 2 Velocities Feet per Minute	Bed 3 Velocities Feet per Minute
A	965	989	580
B	939	868	566
C	913	896	580
D	931	1,013	694
E	760	939	821
F	859	922	760
G	868	1,029	760
H	887	956	877
I	850	997	830
J	1,005	1,037	728
K	840	913	877
L	896	956	760
M	1,005	1,044	749
N	904	904	850
O	896	931	760
P	956	973	537
Q	956	904	552
R	922	877	607

Table B-2. Flow Velocities for the Second 1 3/8-inch Cell [CSC-16-81-38-A (2)]

Sample Location	Bed 1 Velocities Feet per Minute	Bed 2 Velocities Feet per Minute	Bed 3 Velocities Feet per Minute
A	821	896	474
B	850	830	522
C	821	811	607
D	1,005	1,082	760
E	931	896	931
F	801	770	781
G	981	1,021	770
H	939	904	939
I	801	801	850
J	981	1,097	566
K	939	896	716
L	801	811	738
M	1,005	1,021	658
N	859	877	830
O	868	840	749
P	922	956	522
Q	922	896	580
R	896	830	607

Table B-3. Flow Velocities for the First 2-inch Cell [CSC-16-62-A (1)]

Sample Location	Bed 1 Velocities Feet per Minute	Bed 2 Velocities Feet per Minute	Bed 3 Velocities Feet per Minute
A	760	770	420
B	760	705	507
C	770	728	694
D	922	956	658
E	830	840	749
F	811	716	830
G	887	821	580
H	716	749	738
I	749	859	859
J	877	830	682
K	738	770	791
L	801	781	922
M	840	859	552
N	781	749	658
O	801	830	749
P	859	877	522
Q	830	801	580
R	859	877	694

Table B-4. Flow Velocities for the Second 2-inch Cell [CSC-16-62-A (2)]

Sample Location	Bed 1 Velocities Feet per Minute	Bed 2 Velocities Feet per Minute	Bed 3 Velocities Feet per Minute
A	770	791	522
B	728	682	537
C	850	770	694
D	850	859	491
E	728	781	594
F	922	939	728
G	840	887	694
H	896	877	738
I	956	904	840
J	801	821	670
K	716	840	801
L	887	840	859
M	821	830	552
N	749	801	694
O	913	1,005	749
P	821	850	491
Q	859	821	537
R	896	791	694

Table B-5. Flow Breakthrough Locations Test Results

Run No.	Cell Size	Breakthrough Location	Breakthrough Time - minutes	Carbon per Cell - pounds
1	2 inch	G	152	82.5
		A	164	
		D	171	
2	2 inch	G	135	82.5
		A	141	
		D	147	
3	1 3/8 inch	G	68	78
		A	82	
		D	85	
4	1 3/8 inch	G	132	78
		A	136	
		D	140	